THE JOURNAL OF PHYSICAL CHEMISTRY A

Article

pubs.acs.org/JPCA

CIMS Sulfuric Acid Detection Efficiency Enhanced by Amines Due to Higher Dipole Moments: A Computational Study

Oona Kupiainen-Määttä,[†] Tinja Olenius,[†] Theo Kurtén,[‡] and Hanna Vehkamäki[†,*]

[†]Department of Physics, University of Helsinki, P.O. Box 64, FI-00014, Finland

[‡]Department of Chemistry, University of Helsinki, P.O. Box 55, FI-00014, Finland

Supporting Information

ABSTRACT: Quantum chemical calculations have been performed on negatively charged nitric acid−sulfuric acid−dimethylamine clusters. The cluster energies were combined with a kinetic model to study the chemical ionization of sulfuric acid molecules and sulfuric acid−dimethylamine clusters with nitrate ions. Both the sulfuric acid monomer and the $H_2SO_4 \cdot (CH_3)_2NH$ cluster get ionized, but the cluster has a much higher dipole moment, and thus a higher collision rate with charger ions. Clustering of sulfuric acid with bases will therefore increase its detection probability in the CIMS, instead of decreasing it as has been suggested previously. However, our comparison of different quantum chemical methods shows some uncertainty on the extent of sulfuric acid−dimethylamine cluster formation in typical ambient conditions, and no experimental data is available for comparison. Apart from affecting CIMS measurements, the degree of clustering is directly linked to the formation rate of larger clusters, and needs to be quantified in order to understand atmospheric new-particle formation. On the basis of the different charging efficiencies of the monomer and the cluster, a method is proposed for determining experimentally the binding energies of H_2SO_4·base clusters by measuring the extent of cluster formation as a function of base concentration.

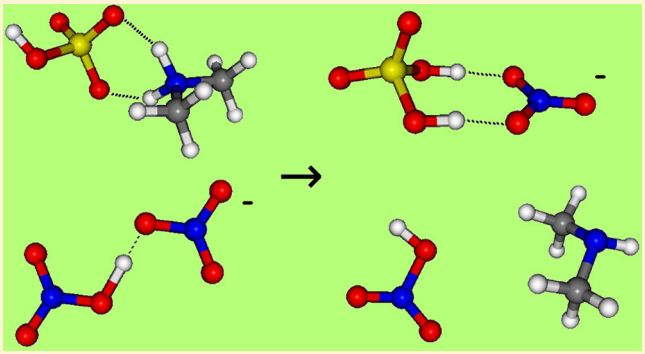

INTRODUCTION

Sulfuric acid has been observed to have an important role in atmospheric new-particle formation in various types of environments around the world.[1,2] Field measurements of gas-phase sulfuric acid started in the 1980s and 1990s when the CIMS (Chemical Ionization Mass Spectrometer) was introduced.[3−5] Since then, the CIMS has been the predominant instrument used for gas-phase sulfuric acid measurements both in field campaigns and in laboratory experiments.

The working principle of the CIMS is to charge the sample gas selectively by chemical ionization, and then detect the ions by mass spectroscopy. In the case of sulfuric acid measurements, the charger ions are typically nitrate ions and/or $HNO_3 \cdot NO_3^-$ dimers. These provide a very selective chemical ionization, as sulfuric acid is one of the only species in the atmosphere that is more acidic than nitric acid. The other compound both commonly present in the atmosphere and charged by nitrate ions is malonic acid.

After the introduction of the CIMS, several studies investigated whether clustering of the charger ions had an effect on the charging efficiency.[6−8] It was concluded that the mass of the charger ion affected the collision frequency as expected, but clustering had no other effect. The impact of cluster formation of the neutral species on the charging efficiency has received less attention until lately, probably at least partly because composition-selective detection of neutral clusters is not possible. Even now, there are no experimental results on formation energies of neutral sulfuric acid−base clusters. Viggiano et al.[8] concluded from their experiments that either $(H_2SO_4)_n$ clusters were not present or did not get ionized by the nitrate ions. Hanson and Eisele[9] suggested that the charging efficiency of $(H_2SO_4)_n \cdot (NH_3)_n$ clusters might be significantly lower than that of pure sulfuric acid due to their lower acidity. Kurtén et al.[10] used quantum chemistry to compute proton transfer energies related to charging sulfuric acid−ammonia and sulfuric acid−dimethylamine clusters with nitrate ions, and concluded that the $H_2SO_4 \cdot NH_3$ and $H_2SO_4 \cdot (CH_3)_2NH$ clusters might have a lower charging probability than sulfuric acid monomers. However, the study was based on equilibrium distributions, and did not take into account the dynamics of the charging process. In the cluster-CIMS[11] and the CI-APi-TOF,[12] charging efficiencies of all clusters have been assumed to be equal to that of sulfuric acid monomers. To our knowledge, charging efficiency estimates have as yet never taken into account the change in the collision rate due to clustering of the neutral molecules.

Several parametrizations have been proposed for collision rates between ions and neutral molecules, the most widely used

Received: May 21, 2013
Revised: December 2, 2013
Published: December 3, 2013

of which are those by Su and Bowers[13] and Su and Chesnavich.[14] Both of these take into account the reduced mass of the collision partners as well as the dipole moment and polarizability of the neutral species. We have used these two parametrizations to calculate collision rates of sulfuric acid and sulfuric acid−dimethylamine clusters with nitrate ions and $HNO_3{\cdot}NO_3^-$ clusters, and computed evaporation rates of the collision products based on three different quantum chemical data sets. We have then simulated the charging process with the cluster collision and evaporation kinetics code ACDC (Atmospheric Cluster Dynamics Code), to obtain results easily comparable with CIMS measurements.

METHODS

Equations Governing Cluster Dynamics. The time evolution of a cluster population can be described by the birth-death equations. The rate of change of each cluster concentration is computed based on collision and fragmentation processes, and possibly external source and loss terms such as chemical reactions or deposition on walls. In this study, the birth-death equations are generated and solved using the Atmospheric Cluster Dynamics Code, ACDC,[15,16] which uses the Matlab ode15s routine[17] for integrating the time evolution.

For neutral-neutral collision rates we use the classical gas kinetics expression

$$\beta_{i,j} = (8\pi k_B T)^{1/2} m_{red}^{-1/2} (r_i + r_j)^2 \quad (1)$$

where m_{red} is the reduced mass of the collision partners, r_i is the radius of cluster i, k_B is the Boltzmann constant, and T is the temperature. The radii are calculated using bulk liquid densities ($\rho_{H_2SO_4}$ = 1830 kg/m^3, ρ_{DMA} = 680 kg/m^3, ρ_{HNO_3} = 1513 kg/m^3)[18] assuming spherical clusters and ideal mixing.

In collisions of ions with neutral molecules or clusters, the collision cross section is larger than would be predicted from the physical dimensions of the collision partners due to their the long-range attraction. A simplified classical treatment of the interaction between the ion and the permanent and induced dipole moment of the neutral species gives the collision frequency[13]

$$\beta_{i,j} = \frac{q_i}{2\varepsilon_0} m_{red}^{-1/2} \left[(4\pi\varepsilon_0 \alpha_j)^{1/2} + C\mu_j \left(\frac{2}{\pi k_B T} \right)^{1/2} \right] \quad (2)$$

where q_i is the charge of the ion, α_j and μ_j are the polarizability and dipole moment of the neutral molecule, respectively, ε_0 is the vacuum permittivity, and $C \in [0,1]$ is an empirical factor scaling the importance of the ion-dipole term. A value of C = 1 would correspond to assuming that the dipole is constantly pointing toward the ion, while a fit to experimental data[13] gave the value C = 0.15 used in this study.

A different approach was presented by Su and Chesnavich[14] who performed trajectory simulations of collisions between a point charge and a rigidly rotating molecule. They observed that the collision frequency depended on three reduced parameters, the Langevin collision rate $\beta_{i,j}^L = q_i m_{red}^{-1/2} (\pi\alpha_j/\varepsilon_0)^{1/2}$, $I^* = \mu_j I/(\alpha_j q m_{red})$ and $x = \mu_j/(8\pi\varepsilon_0\alpha_j k_B T)^{1/2}$, where I is the moment of inertia of the neutral molecule. At low values of I^*, namely when $I^* < (0.7 + x^2)/(2 + 0.6x)$, the collision rate was noted to be independent of I^*, and a fit to the simulated data produced the parametrization

$$\beta_{i,j} = \begin{cases} \beta_{i,j}^L \times (0.4767x + 0.6200), & x \geq 2 \\ \beta_{i,j}^L \times \left(\dfrac{(x + 0.5090)^2}{10.526} + 0.9754 \right), & x < 2 \end{cases} \quad (3)$$

All ion-neutral collisions occurring in this study fall into this low-I^* region.

Both parametrizations have been compared extensively with experimental collision rates and found to give good predictions.[8,19−21] Efforts have also been made to take into account more details such as the kinetic energy of the collision partners[22] or the polarizability of the ion.[23] However, while reaction rates of ion-molecule reactions can readily be measured, it is not always clear if the reactions are collision limited, and experimental assessment of collision rates is less straightforward.[23] In this study, we use mostly the parametrization (3) which has been tested and seen to perform well for nitrate ions and sulfuric acid molecules,[8] but we also present a comparison with parametrization (2) to demonstrate that our conclusions are robust with respect to details in the description of the ion-neutral collision rate.

Evaporation rates of the clusters are calculated assuming detailed balance as[24]

$$\gamma_{i,j} = \frac{P_{ref}}{k_B T} \beta_{i,j} \exp\left[\frac{\Delta G_{i+j} - \Delta G_i - \Delta G_j}{k_B T} \right] \quad (4)$$

where ΔG are the Gibbs free energies of formation of the evaporating cluster and the products at temperature T and pressure P_{ref}.

It is assumed in the simulations that all collisions lead to the formation of the product cluster, and if the product is unfavorable, it is destroyed according to its evaporation rates. The recent experiments by Bzdek et al.[25] suggest that this might not be the case as there may be activation energy barriers related to the collision processes. Although the existence of such barriers seems probable, their height has not yet been quantified. The barriers, if present, are likely to vary between collision partners, and may thus have a different effect on the charging probability of different neutral species. However, while the barriers alter the time evolution of the cluster concentrations, they do not affect the equilibrium distributions as both collision and evaporation rates decrease by the same factor.

Quantum Chemical Calculations. Gibbs free energies of nitric acid containing neutral and negatively charged clusters were calculated using a multistep method presented by Ortega et al.[24] Geometry optimizations and frequency calculations were performed with the B3LYP hybrid functional[26] and a CBSB7 basis set (same as 6-311G(2d,d,p))[27] using the Gaussian09 program,[28] and a higher-level single-point energy was then calculated with the RI-CC2 method[29,30] and an aug-cc-pV(T+d)Z basis set[31] using the TURBOMOLE program.[32] The energies and geometries of the most stable (lowest ΔG) conformers are given at 298.15 K in the Supporting Information and, for the clusters not containing nitric acid, in previous publications.[16,24] For simulations at 278.00 K, the corresponding Gibbs free energies were recalculated based on the vibrational frequencies and rotational constants. The dipole moments and polarizabilities of all neutral molecules and clusters were computed with the B3LYP/CBSB7 method using the Gaussian09 program,[28] and are presented in the Supporting Information. As a comparison, we also use previously

dx.doi.org/10.1021/jp4049764 | J. Phys. Chem. A 2013, 117, 14109−14119

published[10] Gibbs free energies calculated with the G3MP2[33] and PW91/6-311++G(3df, 3pd)[34−36] methods, and in this case the temperature dependence is approximated as $G(T) = H(298.15\ \mathrm{K}) - T{\cdot}S(298.15\ \mathrm{K})$. This gives practically the same result as calculating G from the vibrational frequencies and rotational constants, as both H and S depend weakly on temperature.

G3MP2 is a composite method combining HF/6-31G(d) frequencies (scaled by the factor 0.8929) and a set of electronic energy corrections.[33] It has been tested against experimental enthalpies of formation, ionization energies, electron affinities and proton affinities of a variety of atoms and molecules, and the average absolute deviation from experiment was 1.30 kcal/mol.[33] Similar extensive benchmarking has not been performed for cluster formation energies, and the accuracy of the method is likely to be somewhat worse. One potential problem is that the frequency scaling factor has been optimized for intramolecular vibrations and might not perform as well for frequencies corresponding to the looser intermolecular bonds.

The B3LYP/CBSB7//RICC2/aug-cc-pV(T+d)Z method has been compared with measured formation energies of a few small positively charged sulfuric acid−ammonia clusters and seen to agree well,[21] but a comparison with other quantum chemical methods has suggested that it tends to overestimate the binding of neutral clusters by a few kcal/mol.[37] A comprehensive benchmarking study has not been possible due to the lack of relevant experimental data. The vibrational frequencies are calculated similarly as in the CBS-QB3 method[27] except that the scaling factor 0.99, again optimized for intramolecular vibrations, is not used. Since this part of the calculation is done with a higher level method than the Hartree−Fock calculation used in the G3MP2 method, the frequencies are expected to be more accurate. The electronic energy, however, is simply taken from one RI-CC2 calculation (approximate coupled cluster singles and doubles method, CC2,[29] with the resolution of the identity approximation, RI[30]), while more corrections are taken into account in the G3MP2 method. As a result, it is not clear which of these methods should be trusted more in the context of cluster formation free energies, but at least for the electrically neutral sulfuric acid-DMA clusters the B3LYP/CBSB7//RICC2/aug-cc-pV(T+d)Z method probably gives too negative formation energies.[37]

The pure DFT method PW91/6-311++G(3df, 3pd) with no higher level energy corrections is likely to be less accurate than the other two methods.[37] However, it has been used extensively for sulfuric acid−base−water clusters,[38−40] and was therefore chosen to be included in the comparison.

The only cluster considered in this study for which experimental formation free energies are available is the charger ion trimer $NO_3^-{\cdot}(HNO_3)_2$.[41,42] Enthalpies of formation have been determined also for several other ionic clusters containing sulfuric acid and nitric acid.[43] These formation energies and evaporation rates are compared to the values obtained from different quantum chemical methods in the Supporting Information. Besides the large differences between the three computational methods, also discrepancies between different experiments and between experiments and quantum chemistry are typically of the order of a few kcal/mol for enthalpies and Gibbs free energies or a few orders of magnitude for evaporation rates. Therefore, this comparison does not provide any conclusion about the relative trustworthiness of the computational methods.

A common problem in computing the Gibbs free energy of any complicated system with any standard quantum chemical method is that various kinds of hindered rotations and other large-amplitude motions are treated as harmonic vibrations. The harmonic frequencies obtained for these modes describe the motion poorly no matter how accurate the potential energy surface is, and have a strong effect on the calculated entropy value.[44] On the other hand, reliable experimental determination of cluster formation entropies is also complicated, as illustrated by the very small number of systems for which such information is available. In the quantum-chemical treatment of electronic energies and hence enthalpies, it is essential to take into account electron correlation in order to properly describe chemical bonding and especially weaker interactions such as hydrogen bonding. The most accurate energies are obtained from correlated wavefunction-based methods, and DFT methods are also better than the Hartree−Fock method that completely neglects electron correlation.

Parameters Related to the CIMS. The first step in the operation of the CIMS instrument is to produce nitrate ions. The formed NO_3^- ions then collide with neutral HNO_3 molecules to form $NO_3^-{\cdot}HNO_3$ and $NO_3^-{\cdot}(HNO_3)_2$ clusters. The distribution of these three charger ion types depends on the nitric acid concentration and the charging time, and may vary between different instruments. In the selected ion CIMS (SICIMS[45]) the settings are chosen so that $NO_3^-{\cdot}HNO_3$ clusters are the dominant species with a smaller contribution from NO_3^- ions and an even smaller contribution from $NO_3^-{\cdot}(HNO_3)_2$ clusters. In this study the charger ions are simulated as a mixture of 80% $NO_3^-{\cdot}HNO_3$ clusters and 20% NO_3^- ions.[45]

The formed $NO_3^-{\cdot}(HNO_3)_n$ ions are moved from the ion source to the sample air flow using electric fields, while the neutral HNO_3 molecules are not mixed into the sample air. In field measurements, however, the sampled air itself contains some nitric acid. Daytime ambient nitric acid concentrations have been measured in the range 0.2−20 ppbv.[46−48] The nitric acid in the sample affects the distribution of the charger ions by converting NO_3^- ions to $NO_3^-{\cdot}HNO_3$ clusters, and at very high concentrations also $NO_3^-{\cdot}HNO_3$ to $NO_3^-{\cdot}(HNO_3)_2$. Consequently, the charging efficiency decreases slightly with increasing nitric acid concentration as the mass of the charger ions increases. However, if the instrument is calibrated at the same conditions where the measurements are performed, the variations in the charger ion distribution have little effect unless the charging efficiencies of different clusters are affected very differently (that is, if the neutral clusters have a very wide range of masses). Nitric acid can also form neutral clusters with sulfuric acid and bases, but these have weak binding energies and their concentrations are negligible even at high HNO_3 concentrations. Finally, the nitric acid molecules can collide with the sulfuric acid clusters after charging and thus affect the charged cluster distribution. To demonstrate the effect of the ambient nitric acid concentration, we have studied three different cases: $[HNO_3] = 0$, 0.2, and 20 ppbv.

The concentration of charger ions inside different parts of the instrument is difficult to determine, but it has been estimated[10] to be between 10^6 and 10^9 cm^{-3} in the chemical ionization region. The sulfuric acid concentration measurement is based on the ratio

$$\frac{\sum[HSO_4^-{\cdot}(HNO_3)_n]}{\sum[NO_3^-{\cdot}(HNO_3)_n]}$$

dx.doi.org/10.1021/jp4049764 | J. Phys. Chem. A 2013, 117, 14109−14119

Table 1. Collision Rate Enhancement Due to Clustering, Defined as $\beta_{ion+X}/\beta_{ion+H_2SO_4}$ [a]

	$(HNO_3)_n \cdot NO_3^- + X$					
	eq 2[13]			eq 3[14]		
	$n = 0$	$n = 1$	$n = 2$	$n = 0$	$n = 1$	$n = 2$
cluster (=X)	$\beta_{ion+H_2SO_4} = 1.47 \times 10^{-9}$ cm^3/s	$\beta_{ion+H_2SO_4} = 1.22 \times 10^{-9}$ cm^3/s	$\beta_{ion+H_2SO_4} = 1.13 \times 10^{-9}$ cm^3/s	$\beta_{ion+H_2SO_4} = 2.40 \times 10^{-9}$ cm^3/s	$\beta_{ion+H_2SO_4} = 2.00 \times 10^{-9}$ cm^3/s	$\beta_{ion+H_2SO_4} = 1.85 \times 10^{-9}$ cm^3/s
$H_2SO_4 \cdot H_2O$	0.9	0.9	0.9	0.9	0.8	0.8
$H_2SO_4 \cdot (H_2O)_2$	1.0	1.0	0.9	0.9	0.9	0.9
$H_2SO_4 \cdot (H_2O)_3$	1.0	0.9	0.9	0.8	0.8	0.7
$H_2SO_4 \cdot NH_3$	1.4	1.4	1.4	1.6	1.6	1.5
$H_2SO_4 \cdot (CH_3)_2NH$	2.0	1.9	1.9	2.4	2.4	2.3
$(H_2SO_4)_2$	0.7	0.7	0.6	0.4	0.4	0.4
$(H_2SO_4)_2 \cdot H_2O$	1.5	1.4	1.4	1.6	1.5	1.5
$(H_2SO_4)_2 \cdot (H_2O)_2$	1.6	1.5	1.4	1.7	1.6	1.5
$(H_2SO_4)_2 \cdot (H_2O)_3$	1.7	1.6	1.5	1.9	1.8	1.7
$(H_2SO_4)_2 \cdot NH_3$	2.0	1.9	1.8	2.5	2.3	2.2
$(H_2SO_4)_2 \cdot (CH_3)_2NH$	1.9	1.8	1.7	2.1	2.0	1.9
$(H_2SO_4)_2 \cdot ((CH_3)_2NH)_2$	1.7	1.6	1.5	1.7	1.6	1.5
$H_2SO_4 \cdot (CH_3)_2NH \cdot H_2O$	1.7	1.6	1.6	2.0	1.9	1.8
$H_2SO_4 \cdot (CH_3)_2NH \cdot (H_2O)_2$	1.5	1.4	1.4	1.5	1.5	1.4
$(H_2SO_4)_2 \cdot (CH_3)_2NH \cdot H_2O$	1.7	1.6	1.5	1.8	1.6	1.5

[a]The collision rate $\beta_{ion+H_2SO_4}$ of sulfuric acid with the charger ions $(HNO_3)_n \cdot NO_3^-$ (n = 0, 1, 2) is given in the first row.

which can be determined directly from the mass spectrometer signal counts without knowing the absolute concentrations. This ratio is effectively independent of the initial charger ion concentration, as long as only a small fraction of the charger ions collide with a small fraction of the neutral molecules and clusters. In order to minimize the depletion of neutral sulfuric acid, a charger ion concentration of 10^6 cm^{-3} has been used in this study.

The charger ions are mixed with the sample flow at ambient pressure, and let to react with the neutral molecules and clusters. In the SICIMS,[45] the reaction time is approximately 0.15 s, and this value has been used in the simulations. At the end of the chemical ionization region, the ions are removed from the neutral gas flow using electric fields. The ions are then either guided directly into a mass spectrometer, or first fragmented in a collisional dissociation chamber (CDC) by energetic collisions with neutral molecules. The function of the CDC is to convert all sulfuric acid containing ions into HSO_4^- core ions and all charger ions into NO_3^- core ions, but these fragmentation processes are beyond the scope of this study.

According to quantum chemical calculations, the lowest energy configurations of the clusters $HSO_4^- \cdot HNO_3$ and $HSO_4^- \cdot (HNO_3)_2$ actually have a nitrate ion as charge carrier. A comparison of experimental and theoretical vibrational spectra[49] has shown that the heterodimer can exist both as $HSO_4^- \cdot HNO_3$ and $NO_3^- \cdot H_2SO_4$, while the two heterotrimers correspond predominantly to the structures $NO_3^- \cdot H_2SO_4 \cdot HNO_3$ and $HSO_4^- \cdot H_2SO_4 \cdot HNO_3$. In this study, we assume that all clusters are always in their minimum energy configuration and that all molecules can evaporate from them in their neutral form. This is equivalent to assuming that there are no energy barriers for proton transfers or rearrangement of molecules inside a cluster. With this assumption, the highest evaporation rate from each of these clusters corresponds to HNO_3, and to emphasize this we denote always the bisulfate ion to be the charge carrier.

Cluster Dynamics Simulations. First, the neutral steady-state cluster distribution is simulated with ACDC. When using the B3LYP/CBSB7//RI-CC2/aug-cc-pV(T+d)Z energies, the clusters $(H_2SO_4)_{0-2} \cdot ((CH_3)_2NH)_{0-2}$ are included in the simulation, while for the other quantum chemical methods the $H_2SO_4 \cdot ((CH_3)_2NH)_2$ cluster is left out. For studying the effect of ambient nitric acid, the additional clusters $(H_2SO_4)_{0-1} \cdot ((CH_3)_2NH)_{0-1} \cdot HNO_3$ and $(HNO_3)_2$ are included. A coagulational loss coefficient $L = 2.6 \times 10^{-3}$ s^{-1} corresponding to the Hyytiälä boreal forest station[50] has been used for all molecules and clusters. In all neutral cluster simulations, the DMA concentration and either the sum $[H_2SO_4] + [H_2SO_4 \cdot (CH_3)_2NH]$ or the sulfuric acid production rate are set to a constant value, and all other concentrations are initially set to zero. The birth-death equations are then integrated until a steady state is reached.

According to a previous study using B3LYP/CBSB7//RI-CC2/aug-cc-pV(T+d)Z energies,[16] the principal growth route to clusters with more than two sulfuric acid molecules is through a collision of $(H_2SO_4)_2 \cdot ((CH_3)_2NH)_2$ with $H_2SO_4 \cdot (CH_3)_2NH$. Therefore, clusters are allowed to grow out of the current simulation system only via collisions that lead to clusters containing at least three sulfuric acids and three DMAs. This boundary condition also reproduces the cluster distribution found in a system of clusters up to $(H_2SO_4)_4 \cdot ((CH_3)_2NH)_4$ better than if clusters are allowed to grow out with only three acids and two DMAs. When collisions produce clusters that are outside the simulated system but do not fulfill the condition for growing out of the system, they are assumed to evaporate molecules instantaneously until they are back in the system. For instance a collision of two $(H_2SO_4)_2 \cdot (CH_3)_2NH$ clusters will result in a $(H_2SO_4)_2 \cdot ((CH_3)_2NH)_2$ cluster and two H_2SO_4 molecules. When nitric acid containing clusters are used, any nitric acid molecules are evaporated first when bringing a collision product back into the system. A more detailed description of growth pathways and boundary conditions can be found in our earlier publication.[16]

After obtaining the neutral cluster distribution, we move on to the chemical ionization. The flow is assumed to be locally well mixed, so that concentrations are well-defined and the

dx.doi.org/10.1021/jp4049764 | J. Phys. Chem. A 2013, 117, 14109−14119

Table 2. Evaporation Rates (1/s) at T = 298.15 K Calculated Using Eqs 4 and 3 and B3LYP/CBSB7//RICC2/aug-cc-pV(T+d)Z Cluster Energies and B3LYP/CBSB7 Dipole Moments and Polarizabilities[a]

	evaporating molecule		
cluster	H_2SO_4	$(CH_3)_2NH$	HNO_3
$H_2SO_4 \cdot (CH_3)_2NH$	**5.9×10^{-2}**	**5.9×10^{-2}**	
$(H_2SO_4)_2$	**7.1×10^{3}**		
$(H_2SO_4)_2 \cdot (CH_3)_2NH$	**5.5×10^{-5}**	2.2×10^{-10}	
$(H_2SO_4)_2 \cdot ((CH_3)_2NH)_2$	1.5×10^{-15}	**9.8×10^{-5}**	
$HSO_4^- \cdot (CH_3)_2NH$		**7.5×10^{9}**	
$HSO_4^- \cdot H_2SO_4$	**2.6×10^{-15}**		
$HSO_4^- \cdot H2SO_4 \cdot (CH_3)_2NH$	1.7×10^{-22}	**4.8×10^{2}**	
$HSO_4^- \cdot H_2SO_4 \cdot ((CH_3)_2NH)_2$		**3.5×10^{8}**	
$NO_3^- \cdot HNO_3$			**9.6×10^{-8}**
$NO_3^- \cdot (HNO_3)_2$			**2.3×10^{5}**
$HSO_4^- \cdot HNO_3$	1.1×10^{-15}		**3.2×10^{-4}**
$HSO_4^- \cdot (HNO_3)_2$	1.1×10^{-3}		**9.6×10^{4}**
$HSO_4^- \cdot HNO_3 \cdot (CH_3)_2NH$		**2.6×10^{3}**	1.1×10^{-10}
$HSO_4^- \cdot (HNO_3)_2 \cdot (CH_3)_2NH$		4.4×10^{2}	**1.7×10^{4}**
$(HNO_3)_2$			**2.9×10^{11}**
$H_2SO_4 \cdot HNO_3$	**1.6×10^{8}**		**1.6×10^{8}**
$HNO_3 \cdot (CH_3)_2NH$		**3.5×10^{5}**	**3.5×10^{5}**
$H_2SO_4 \cdot HNO_3 \cdot (CH_3)_2NH$	1.0×10^{-2}	2.0×10^{-5}	**6.2×10^{4}**
$HSO_4^- \cdot H_2SO_4 \cdot HNO_3$	6.7×10^{-7}		**8.2×10^{4}**
$HSO_4^- \cdot H_2SO_4 \cdot HNO_3 \cdot (CH_3)_2NH$	8.7×10^{-11}	3.3×10^{-1}	**5.7×10^{1}**
$HSO_4^- \cdot H_2SO_4 \cdot (HNO_3)_2 \cdot (CH_3)_2NH$	3.4×10^{-9}		**6.4×10^{5}**
$HSO_4^- \cdot H_2SO_4 \cdot HNO_3 \cdot ((CH_3)_2NH)_2$		**6.9**	1.1×10^{-6}
$HSO_4^- \cdot H_2SO_4 \cdot (HNO_3)_2 \cdot ((CH_3)_2NH)_2$		5.1×10^{-1}	**4.7×10^{4}**

[a]The highest evaporation rate for each cluster is marked in bold.

birth-death equations can be used. We sum up the neutral distribution and the charger ions ($[NO_3^-] = 2 \times 10^5$ cm^{-3} and $[NO_3^- \cdot HNO_3] = 8 \times 10^5$ cm^{-3}) to give the initial concentration, and then run the simulation for 0.15 s with no additional source terms. Since the wall losses inside the instrument are not known, we use for neutrals the same losses as in the neutral simulation and for ions the same value multiplied by a factor of 2. The sets of clusters used with each quantum chemical method are presented in Tables 2–4. For G3MP2 and PW91/6-311++G(3df,3pd), negative clusters with two sulfuric acids and one or more nitric acids are not available, so we concentrate mainly on the B3LYP/CBSB7//RI-CC2/aug-cc-pV(T+d)Z data in the chemical ionization simulations. The negative clusters are allowed to grow out of the system if they contain at least three sulfuric acid molecules. Otherwise, collision products outside the simulated system are forced back into the system by evaporating nitric acid and DMA molecules.

RESULTS

Collision and Evaporation Rates. The collision rates of sulfuric acid molecules and neutral sulfuric acid containing clusters with the charger ions NO_3^-, $NO_3^- \cdot HNO_3$ and $NO_3^- \cdot (HNO_3)_2$ were calculated using eqs 2 and 3. The dipole moments and polarizabilities used for the collision rates were calculated with the B3LYP/CBSB7 method, and they are presented in the Supporting Information. The collision enhancement factors due to clustering, β(ion + X)/β(ion + H_2SO_4), are presented in Table 1. The two methods of Su and Bowers[13] and Su and Chesnavich[14] give somewhat different values for the collision rates, but both predict similar trends with respect to clustering.

It can be seen that hydration of the sulfuric acid molecule has very little effect on its collision rate with the charger ions. On the other hand, clustering with a DMA molecule increases the collision rate by a factor of 2 due to the significant (factor of 3) increase in the dipole moment. If the $H_2SO_4 \cdot (CH_3)_2NH$ cluster is hydrated, the collision enhancement is slightly smaller but still significant. Clustering with ammonia also increases the collision rate, but the $H_2SO_4 \cdot NH_3$ cluster is less stable and therefore less abundant than the $H_2SO_4 \cdot (CH_3)_2NH$ cluster.

The pure sulfuric acid dimer is very symmetric and thus has a small dipole moment and a low collision rate with ions. It is, however, quite unstable (i.e., has a very high evaporation rate) according to all quantum chemical methods, and has a negligible concentration at ambient conditions. Addition of water or ammonia molecules to the acid dimer increases its dipole moment and also stabilizes it, but not enough to make it abundant compared to the monomer in conditions relevant for the boundary layer.[51] DMA, on the other hand, forms strongly bound clusters with two sulfuric acid molecules, and these clusters, both dry and hydrated, have high dipole moments and a strong collision enhancement compared to the sulfuric acid monomer.

In both parametrizations (2) and (3), the only effect of the identity of the charger ion on the collision rate is through its mass. The collision enhancement factor for each neutral cluster decreases slightly as the mass of the charger ion increases, but overall the composition of the neutral cluster has a stronger effect on the enhancement factor than the size of the charger ion.

From here on, we concentrate on sulfuric acid–DMA clusters. These are predicted by the two most reliable quantum chemical methods used in this study to be abundant even at trace concentrations of DMA. Recent experimental results[51] also show a strong effect of ppt-level DMA on sulfuric acid cluster formation, indicating significant formation of small

dx.doi.org/10.1021/jp4049764 | J. Phys. Chem. A 2013, 117, 14109–14119

Table 3. Evaporation Rates (1/s) at T = 298.15 K Calculated Using Eqs 4 and 3 with G3MP2 Cluster Energies[10] and B3LYP/CBSB7 Dipole Moments and Polarizabilities[a]

	evaporating molecule		
cluster	H_2SO_4	$(CH_3)_2NH$	HNO_3
$H_2SO_4 \cdot (CH_3)_2NH$	**1.4**	**1.4**	
$(H_2SO_4)_2$	**1.6×10^{4}**		
$(H_2SO_4)_2 \cdot (CH_3)_2NH$	**5.6×10^{-5}**	2.3×10^{-9}	
$(H_2SO_4)_2 \cdot ((CH_3)_2NH)_2$		**2.1×10^{-4}**	
$HSO_4^- \cdot (CH_3)_2NH$		**4.6×10^{9}**	
$HSO_4^- \cdot H_2SO_4$	**1.2×10^{-14}**		
$HSO_4^- \cdot H_2SO_4 \cdot (CH_3)_2NH$	3.3×10^{-20}	**1.2×10^{4}**	
$HSO_4^- \cdot H_2SO_4 \cdot ((CH_3)_2NH)_2$		**3.0×10^{9}**	
$NO_3^- \cdot HNO_3$			**1.8×10^{-5}**
$HSO_4^- \cdot HNO_3$	1.7×10^{-13}		**7.8×10^{-3}**
$HSO_4^- \cdot (HNO_3)_2$	4.7×10^{-6}		**5.2×10^{2}**
$HSO_4^- \cdot HNO_3 \cdot (CH_3)_2NH$		**1.8×10^{5}**	3.0×10^{-7}
$HSO_4^- \cdot (HNO_3)_2 \cdot (CH_3)_2NH$		**1.4×10^{3}**	4.2

[a]The highest evaporation rate for each cluster is marked in bold.

Table 4. Evaporation Rates (1/s) at T = 298.15 K Calculated Using Eqs 4 and 3 with PW91/6-311++G(3df,3pd) Cluster Energies[10] and B3LYP/CBSB7 Dipole Moments and Polarizabilities[a]

	evaporating molecule		
cluster	H_2SO_4	$(CH_3)_2NH$	HNO_3
$H_2SO_4 \cdot (CH_3)_2NH$	**2.4×10^{1}**	**2.4×10^{1}**	
$(H_2SO_4)_2$	**4.7×10^{4}**		
$(H_2SO_4)_2 \cdot (CH_3)_2NH$	**7.6×10^{-2}**	1.9×10^{-5}	
$(H_2SO_4)_2 \cdot ((CH_3)_2NH)_2$		**2.1×10^{3}**	
$HSO_4^- \cdot (CH_3)_2NH$		**9.5×10^{10}**	
$HSO_4^- \cdot H_2SO_4$	**6.1×10^{-14}**		
$HSO_4^- \cdot H_2SO_4 \cdot (CH_3)_2NH$	2.0×10^{-17}	**3.1×10^{7}**	
$HSO_4^- \cdot H_2SO_4 \cdot ((CH_3)_2NH)_2$		**6.9×10^{11}**	
$NO_3^- \cdot HNO_3$			**2.4×10^{-7}**
$NO_3^- \cdot (HNO_3)_2$			**3.1×10^{3}**
$HSO_4^- \cdot HNO_3$	1.0×10^{-15}		**5.7×10^{-5}**
$HSO_4^- \cdot (HNO_3)_2$	3.0×10^{-4}		**7.1×10^{4}**
$HSO_4^- \cdot HNO_3 \cdot (CH_3)_2NH$		**1.5×10^{10}**	9.1×10^{-6}
$HSO_4^- \cdot (HNO_3)_2 \cdot (CH_3)_2NH$		**4.2×10^{7}**	2.0×10^{2}

[a]The highest evaporation rate for each cluster is marked in bold.

sulfuric acid−amine clusters. Furthermore, the H_2SO_4·DMA clusters have a relatively high ion collision enhancement with respect to sulfuric acid monomers, and thus provide an interesting test case. Other strong bases are likely to behave in a similar way. As hydration of the neutral clusters and charger ions affects the collision rates and cluster distributions only slightly, the presence of water does not change qualitatively the effect of DMA on the detection of sulfuric acid, and for simplicity we only consider dry clusters.

Evaporation rates calculated according to eqs 4, 1, and 3 and using formation free energies computed with the B3LYP/CBSB7//RI-CC2/aug-cc-pV(T+d)Z method are presented in Table 2. In the simulations, clusters are also allowed to break into two smaller clusters, but these fission rates are lower than the highest monomer evaporation rates.

As a comparison, evaporation rates calculated from previously published cluster energies using different quantum chemical methods[10] are presented in Tables 3 and 4. The same collision rates have been used in all cases to enable direct evaluation of the differences due to the different binding energies predicted by different methods. In any case, while the dipole moments and polarizabilities affect the evaporation rates via detailed balance, the free energies are by far the determining factor.

The evaporation rates obtained using B3LYP/CBSB7//RI-CC2/aug-cc-pV(T+d)Z energies and G3MP2 energies are mostly within 2 orders of magnitude of each other, while PW91/6-311++G(3df,3pd) evaporation rates differ more from the two other sets. The largest discrepancy between the different methods is in the $(H_2SO_4)_2 \cdot ((CH_3)_2NH)_2$ cluster, which is predicted to be very unstable according to the PW91/6-311++G(3df,3pd) method and very stable according to the two other methods. Overall, B3LYP/CBSB7//RI-CC2/aug-cc-pV(T+d)Z predicts strongest binding, G3MP2 slightly weaker binding and PW91/6-311++G(3df,3pd) much weaker binding. G3MP2 is the highest level quantum chemistry method of this set, but since none of the methods have been designed for molecular clusters, it is not certain whether it is closest to the true formation energy for all clusters. Therefore, cluster kinetics simulations have been performed with all three sets of quantum chemical cluster energies.

Cluster Distributions before and after Chemical Ionization. *Neutral Cluster Distributions.* Neutral steady state cluster distributions at different conditions and calculated

dx.doi.org/10.1021/jp4049764 | J. Phys. Chem. A 2013, 117, 14109−14119

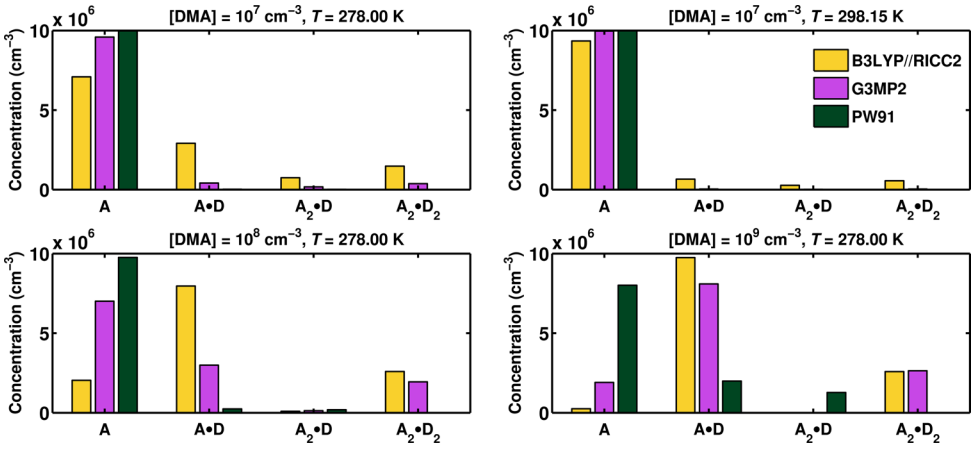

Figure 1. Neutral cluster distributions calculated using B3LYP/CBSB7//RICC2/aug-cc-pV(T+d)Z (yellow), G3MP2 (purple), and PW91/6-311++G(3df,3pd) (green) cluster energies. In the cluster names, A is sulfuric acid and D is DMA. In all panels, the sum of concentrations of sulfuric acid monomers and $H_2SO_4 \cdot (CH_3)_2NH$ clusters is 10^7 cm^{-3}. The DMA concentrations 10^7, 10^8, and 10^9 cm^{-3} are approximately 0.4, 4, and 40 pptv, respectively.

with the three sets of cluster energies are presented in Figure 1. First of all, the figure shows that the different quantum chemical methods give very different predictions. While all methods agree that at room temperature and sub pptv levels of DMA most sulfuric acid is in free molecular form and that $H_2SO_4 \cdot (CH_3)_2NH$ cluster concentrations become non-negligible at low temperatures and high DMA concentrations, the predicted cluster distributions differ strongly at conditions relevant, for instance, to spring-time new-particle formation in a boreal forest. At T = 278 K, $[H_2SO_4] + [H_2SO_4 \cdot (CH_3)_2NH] = 10^7$ cm^{-3} and [DMA] ≈ 4 pptv, the clustering fraction $[H_2SO_4 \cdot (CH_3)_2NH]/([H_2SO_4] + [H_2SO_4 \cdot (CH_3)_2NH])$ is 80%, 30% and 2% according to the B3LYP/CBSB7//RICC2/aug-cc-pV(T+d)Z, G3MP2 and PW91/6-311++G(3df,3pd) methods, respectively. The methods also disagree on the extent of formation of two-acid clusters and whether these clusters contain one or two DMA molecules.

Correct understanding of the formation energetics of small sulfuric acid-containing clusters is crucial for understanding the first steps of atmospheric new-particle formation. Since quantum chemical methods cannot, at present, give a definitive answer, it would be important to study the acid-base binding energies experimentally.

Cluster Distributions after Chemical Ionization. Cluster distributions before and after chemical ionization are presented in Figure 2 for the B3LYP/CBSB7//RICC2/aug-cc-pV(T+d)Z quantum chemical data. Both sulfuric acid monomers and $H_2SO_4 \cdot (CH_3)_2NH$ clusters form $HSO_4^- \cdot HNO_3$ clusters when colliding with any $NO_3^- \cdot (HNO_3)_{0-2}$ charger ions, as the DMA as well as the second and third nitric acid molecules evaporate almost immediately. The charging efficiency is the higher the more $H_2SO_4 \cdot (CH_3)_2NH$ clusters are present, since they have a higher collision rate with the charger ions than pure acid monomers. The collision rates of clusters containing two sulfuric acid molecules with the charger ions are between those of the acid molecule and the $H_2SO_4 \cdot (CH_3)_2NH$ cluster, which means that the ratio of two-sulfuric-acid-species to one-sulfuric-acid-species increases upon charging, unless $H_2SO_4 \cdot (CH_3)_2NH$ clusters dominate strongly over H_2SO_4 monomers. After ionization, the $HSO_4^- \cdot H_2SO_4$ dimer is the most stable two-sulfuric-acid-cluster, but the lifetimes of $HSO_4^- \cdot H_2SO_4 \cdot HNO_3 \cdot (CH_3)_2NH$ and $HSO_4^- \cdot H_2SO_4 \cdot HNO_3 \cdot ((CH_3)_2NH)_2$ are 30

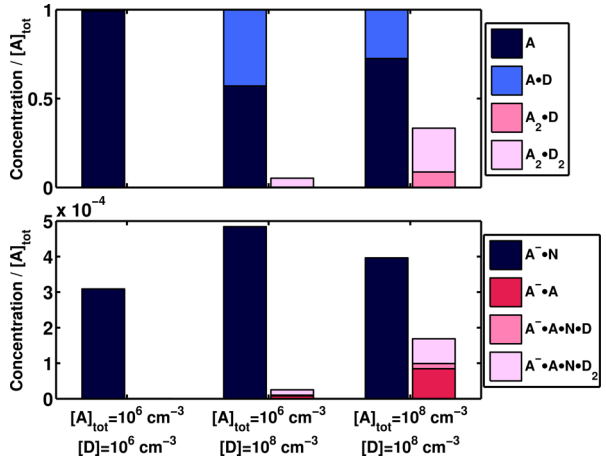

Figure 2. Charging efficiencies at T = 298.15 K and $[HNO_3]$ = 0.2 ppbv. The upper panel shows neutral cluster distributions at different sulfuric acid and DMA concentrations, and the lower panel shows the distribution of negatively charged sulfuric acid clusters after chemical ionization. A, A$^-$, D and N refer to sulfuric acid, bisulfate ion, DMA and nitric acid, respectively, and $[A]_{tot}$ is the sum of free H_2SO_4 and $H_2SO_4 \cdot (CH_3)_2NH$ clusters. The evaporation rates correspond to the B3LYP/CBSB7//RICC2/aug-cc-pV(T+d)Z cluster energies.

and 150 ms, respectively, and these may therefore survive into the mass spectrometer. If, however, the clusters are fragmented in a CDC after chemical ionization, the $HSO_4^- \cdot HNO_3$ clusters (blue bars in the lower panel of Figure 1) are probably detected as HSO_4^- ions and all the two-sulfuric-acid-containing-clusters (red bars) as either $HSO_4^- \cdot H_2SO_4$ or HSO_4^- ions.

The charging process is described very similarly by all quantum chemical methods. According to the G3MP2 and PW91/6-311++G(3df,3pd) methods, the $HSO_4^- \cdot (HNO_3)_2 \cdot (CH_3)_2NH$ cluster loses first a DMA and then a nitric acid, while for B3LYP/CBSB7//RICC2/aug-cc-pV(T+d)Z the order is opposite, but in any case both H_2SO_4 and $H_2SO_4 \cdot (CH_3)_2NH$ become $HSO_4^- \cdot HNO_3$ clusters upon charging. Energies of clusters containing two sulfuric acid molecules and nitric acid are not available with the other methods, but all methods agree that the $HSO_4^- \cdot H_2SO_4$ dimer is very stable and that DMA does not bind to it.

dx.doi.org/10.1021/jp4049764 | J. Phys. Chem. A 2013, 117, 14109−14119

Nitric acid present in the sample does not affect the operation of the CIMS significantly. All neutral nitric acid containing clusters have high evaporation rates, and even at high levels of nitric acid their concentrations are negligible. The nitric acid concentration affects the charger ion distribution and, as the dimer and trimer have lower collision rates with neutral molecules and clusters, a higher nitric acid concentration leads to a slightly lower charging probability. A high nitric acid concentration can also increase the amount of DMA and nitric acid molecules remaining in the clusters after chemical ionization as shown in Figure 3. However, if the CDC

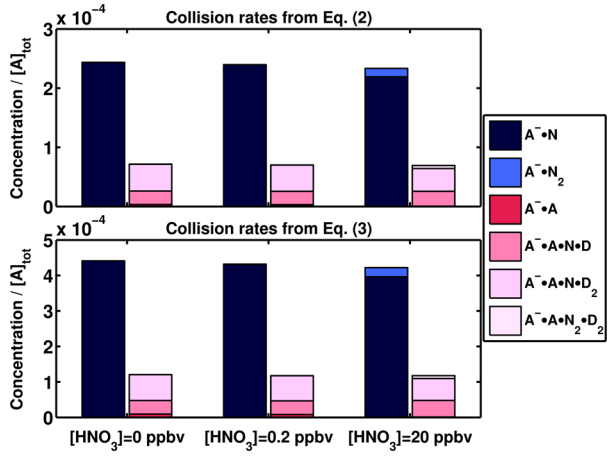

Figure 3. Charging efficiencies at T = 278.00 K and different nitric acid concentrations. The sulfuric acid concentration $[H_2SO_4]$ + $[H_2SO_4{\cdot}(CH_3)_2NH]$ and the DMA concentration are both 10^7 cm^{-3}. The corresponding neutral cluster distribution is shown in the upper left panel of Figure (1). In the upper panel the ion-neutral collision rates are calculated according to eq 2 and in the lower panel according to eq 3. Cluster energies are calculated with the B3LYP/CBSB7//RICC2/aug-cc-pV(T+d)Z method. A, A$^-$, D, and N refer to sulfuric acid, bisulfate ion, DMA, and nitric acid, respectively.

removes efficiently all nitric acid and DMA molecules from the clusters, the main effect of nitric acid is via changes in the charger ion distribution, and this can be minimized by calibrating the instrument at the measurement site, as is typically done.

Figure 3 shows also a comparison between the two parametrizations for the ion-neutral collision rate. Equation 3 gives an overall higher charging probability, while eq 2 predicts a higher ratio of two-sulfuric-acid-clusters to one-sulfuric-acid clusters in the charged distribution. At low nitric acid concentrations eq 3 results in more pure $HSO_4^-{\cdot}H_2SO_4$ dimers relative to clusters with two sulfuric acids and DMA and nitric acid, and this effect is more pronounced at higher temperatures. Finally, eq 3 predicts a higher charging enhancement for the $H_2SO_4{\cdot}(CH_3)_2NH$ cluster compared to the pure acid monomer, as seen in Table 1.

Suggestion for Experimental Determination of Acid-Base Cluster Formation Energies. The higher charging probability of the $H_2SO_4{\cdot}(CH_3)_2NH$ cluster compared to the H_2SO_4 monomer can be used for determining the ratio of pure sulfuric acid molecules and molecules bound to DMA. The binding fraction will then yield the equilibrium constant of the clustering process, and through this the binding energy of the cluster. Here we present the framework for the proposed experiment.

The aim is to make several measurements with a fixed total amount of sulfuric acid and a varying DMA concentration, and study the partitioning of sulfuric acid between free monomers and $H_2SO_4{\cdot}(CH_3)_2NH$ clusters. In order to keep the sum of the concentrations of these compounds constant, the measurements should be carried out at a low enough sulfuric acid concentration or high enough temperature that the particle formation rate remains negligible at all DMA concentrations. If the sulfuric acid source rate is too high, the addition of DMA will lead to the formation of larger sulfuric acid−DMA clusters and a decrease in the sum of H_2SO_4 monomers and $H_2SO_4{\cdot}(CH_3)_2NH$ clusters. A chamber experiment is preferable to a flow tube experiment to ensure that the cluster formation reaches equilibrium. Establishing a constant acid concentration into an empty chamber takes some tens of minutes, and when DMA is then added incrementally, for instance increasing the concentration by a factor of 10 at each step, the system gets close to the new equilibrium within a few minutes for each DMA value. If the experiment is repeated at different temperatures, the enthalpic (H) and entropic (S) contributions to the Gibbs free energy can be solved from the relation $G(T) = H - TS$, assuming that H and S are approximately independent of temperature.

The upper panel of Figure 4 shows the simulated steady-state concentrations of the sulfuric acid monomer and $H_2SO_4{\cdot}$

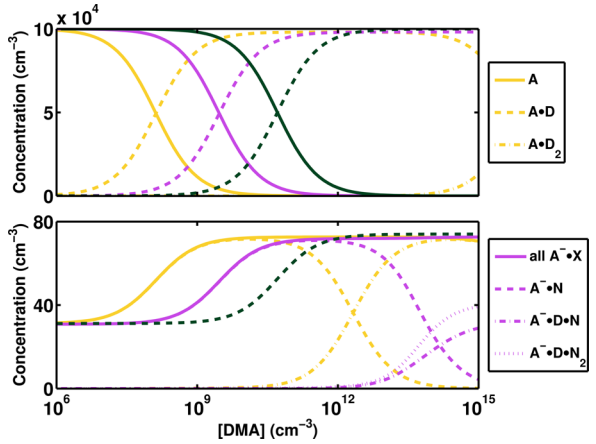

Figure 4. Upper panel: simulated concentrations of H_2SO_4 monomers and $H_2SO_4{\cdot}DMA_{1-2}$ clusters at T = 298.15 K as a function of DMA concentration while the sulfuric acid source term is kept constant. Lower panel: simulated ion concentrations after chemical ionization of the distribution in the upper panel. A, A$^-$, D, and N refer to sulfuric acid, bisulfate ion, DMA, and nitric acid, respectively. The yellow, purple, and green lines correspond to B3LYP/CBSB7//RICC2/aug-cc-pV(T+d)Z, G3MP2, and PW91/6-311++G(3df,3pd) cluster energies, respectively.

$((CH_3)_2NH)_{1-2}$ clusters as a function of DMA concentration according to the three different quantum chemical methods. The sulfuric acid source term is constant, and at a low DMA concentration all sulfuric acid is as free monomers. When the DMA concentration increases, an increasing fraction of the sulfuric acid binds to it, until finally all the sulfuric acid is in $H_2SO_4{\cdot}(CH_3)_2NH$ clusters. The DMA concentration required for this transition depends on the binding energy of the cluster.

The simulated charged cluster distribution after chemical ionization is shown in the lower panel of Figure 4. The ion signal in the CIMS increases as more sulfuric acid is bound to DMA, and the midpoint between the low-DMA signal

dx.doi.org/10.1021/jp4049764 | J. Phys. Chem. A 2013, 117, 14109−14119

corresponding to only sulfuric acid monomers and the high-DMA signal corresponding to only $H_2SO_4 \cdot (CH_3)_2NH$ clusters gives the DMA concentration $[DMA]_{0.5}$ at which half of the sulfuric acid is bound to DMA. According to the equilibrium condition

$$\gamma_{H_2SO_4,DMA}[H_2SO_4 \cdot DMA] = \beta_{H_2SO_4,DMA}[H_2SO_4][DMA]$$

the DMA concentration $[DMA]_{0.5}$ at which $[H_2SO_4 \cdot (CH_3)_2NH] = [H_2SO_4]$ is

$$[DMA]_{0.5} = \frac{\gamma_{H_2SO_4,DMA}}{\beta_{H_2SO_4,DMA}} = \frac{P_0}{k_B T} \frac{1}{K_{H_2SO_4,DMA}}$$

where P_0 is the standard pressure and $K_{H_2SO_4,DMA}$ is the equilibrium constant for the formation of the $H_2SO_4 \cdot (CH_3)_2NH$ cluster. This can further be expressed in terms of the cluster formation free energy as

$$\Delta G(H_2SO_4 \cdot DMA) = k_B T \ln\left(\frac{k_B T [DMA]_{0.5}}{P_{ref}}\right) \quad (5)$$

where P_{ref} is the pressure at which the Gibbs free energy is evaluated. This simplified treatment assumes that the sulfuric acid source term and the external losses can be neglected. The full expression for the steady state condition for the monomer concentration is

$$\frac{d[H_2SO_4]}{dt} = -\beta_{H_2SO_4,DMA}[H_2SO_4][DMA] + \gamma_{H_2SO_4,DMA}[H_2SO_4 \cdot DMA] + Q_{H_2SO_4} - L_{H_2SO_4}[H_2SO_4] = 0$$

where $Q_{H_2SO_4}$ is the source term and $L_{H_2SO_4}$ is the loss constant, and the corresponding equation for the cluster formation energy is

$$\Delta G(H_2SO_4 \cdot DMA) = k_B T \ln\left\{\frac{k_B T}{P_{ref}}\left([DMA]_{0.5} - \frac{Q_{H_2SO_4}}{\beta_{H_2SO_4,DMA}[H_2SO_4]_{0.5}} + \frac{L_{H_2SO_4}}{\beta_{H_2SO_4,DMA}}\right)\right\} \quad (6)$$

where $[H_2SO_4]_{0.5} = {}^1/_2[H_2SO_4]_{tot}$ is the sulfuric acid monomer concentration at the DMA concentration $[DMA]_{0.5}$. In the simulations of Figure 4, we have assumed a wall loss equal to the coagulation sink used in the other simulations, $L_{H_2SO_4} = L_{H_2SO_4 \cdot DMA} = 2.6 \times 10^{-3}\ s^{-1}$, which leads to a correction of $-5.75 \times 10^6\ cm^{-3}$ to the DMA concentration (second and third term in the brackets in eq 6). The midpoint DMA concentrations $[DMA]_{0.5}$ are 1.3×10^8, 3.0×10^9 and $5.1 \times 10^{10}\ cm^{-3}$ according to the B3LYP/CBSB7//RICC2/aug-cc-pV(T+d)Z, G3MP2 and PW91/6-311++G(3df,3pd) cluster energies, respectively, so eq 5 can safely be used. If, however, the estimated correction terms due to losses are of the same order as the measured midpoint DMA concentration, it may be difficult to estimate accurately the binding energy.

It should be noted that eq 5 remains unchanged even if the cluster formation involves a kinetic barrier, as the collision and evaporation rates decrease by the same factor. On the other hand, the correction term in eq 6 depends explicitly on the collision rate and is thus affected by the barrier, so the validity of eq 5 might be difficult to assess. However, the correction term is in any case negative, so eq 5 provides always an upper limit for the cluster formation energy.

CONCLUSIONS

We have modeled the charging of sulfuric acid molecules and small sulfuric acid−dimethylamine clusters in a chemical ionization mass spectrometer (CIMS) using the cluster collision and evaporation code ACDC (atmospheric cluster dynamics code). As input, we used three sets of quantum chemical cluster formation energies and two parametrizations for ion-neutral collision rates.

All three quantum chemical methods agree that upon colliding with $NO_3^- \cdot (HNO_3)_{0-1}$ charger ions both H_2SO_4 monomers and $H_2SO_4 \cdot (CH_3)_2NH$ clusters form $HSO_4^- \cdot HNO_3$ ions within a few milliseconds. Furthermore, both collision rate parametrizations agree that neutral clusters with a high dipole moment have higher collision rates with the charger ions than neutral molecules that have a lower mass and lower dipole moment. Acid-base pairs typically have a high dipole moment, as either the acid donates a proton to the base to form an ion pair, or in the case of weaker acids and bases the base donates an electron pair to the acid, which also leads to charge separation within the cluster. Therefore, clustering of sulfuric acid with base molecules is predicted to enhance its detection in the CIMS, instead of hindering it as has been suggested previously based on equilibrium cluster distributions.

The formation of H_2SO_4·base clusters is the first step in the formation of larger acid-base clusters and finally aerosol particles. While two out of the three quantum chemical methods used in this study suggest that a large fraction of gas-phase sulfuric acid is bound to amines at atmospherically relevant conditions, the magnitude of the formation energy and the extent of the formation of these clusters remain unclear, and experiments are needed to resolve the question. In this article, we have suggested a simple experiment for measuring the formation energy of H_2SO_4·base clusters using the difference in charging efficiencies between the acid monomer and the cluster.

ASSOCIATED CONTENT

Supporting Information

Quantum chemical cluster formation energies, dipole moments, polarizabilities and coordinates. This material is available free of charge via the Internet at http://pubs.acs.org/.

AUTHOR INFORMATION

Corresponding Author

*(H.V.) E-mail: hanna.vehkamaki@helsinki.fi. Telephone: +358 (0)40 560 8807. Fax: +358 (0)9 191 50860.

Notes

The authors declare no competing financial interest.

ACKNOWLEDGMENTS

This work was supported by ERC Projects 257360-MOCAPAF and 27463-ATMNUCLE, Vilho, Yrjö and Kalle Väisälä Foundation, and Academy of Finland LASTU Program, Project Number 135054. We thank CSC−IT Center for Science in Espoo, Finland, for computing time.

REFERENCES

(1) Sihto, S.-L.; Kulmala, M.; Kerminen, V.-M.; Maso, M. D.; Petäjä, T.; Riipinen, I.; Korhonen, H.; Arnold, F.; Janson, R.; Boy, M.; et al. Atmospheric sulphuric acid and aerosol formation: Implications from atmospheric measurements for nucleation and early growth mechanisms. *Atmos. Chem. Phys.* **2006**, *6*, 4079−4091.

(2) Kuang, C.; McMurry, P. H.; McCormick, A. V.; Eisele, F. L. Dependence of nucleation rates on sulfuric acid vapor concentration in diverse atmospheric locations. *J. Geophys. Res.* **2008**, *113*, D10209.

(3) Arnold, F.; Fabian, R.; Joos, W. Measurements of the height variation of sulfuric acid vapor concentrations in the stratosphere. *Geophys. Res. Lett.* **1981**, *8*, 293−296.

(4) Viggiano, A. A.; Arnold, F. Extended sulfuric acid vapor concentration measurements in the stratosphere. *Geophys. Res. Lett.* **1981**, *8*, 583−586.

(5) Eisele, F.; Tanner, D. Measurement of the gas phase concentration of H_2SO_4 and methane sulfonic acid and estimates of H_2SO_4 production and loss in the atmosphere. *J. Geophys. Res.* **1993**, *98*, 9001−9010.

(6) Viggiano, A. A.; Perry, R. A.; Albritton, D. L.; Ferguson, E. E.; Fehsenfeld, F. C. Stratospheric negative-ion reaction rates with H_2SO_4. *J. Geophys. Res.* **1982**, *87*, 7340−7342.

(7) Tanner, D. J.; Eisele, F. L. Present OH measurement limits and associated uncertainties. *J. Geophys. Res.* **1995**, *100*, 2883−2892.

(8) Viggiano, A. A.; Seeley, J. V.; Mundis, P. L.; Williamson, J. S.; Morris, R. A. Rate Constants for the Reactions of $XO_3^-(H_2O)_n$ (X = C, HC, and N) and $NO_3^-(HNO_3)_n$ with H_2SO_4: Implications for Atmospheric Detection of H_2SO_4. *J. Phys. Chem. A* **1997**, *101*, 8275−8278.

(9) Hanson, D. R.; Eisele, F. L. Measurement of prenucleation molecular clusters in the NH_3, H_2SO_4, H_2O system. *J. Geophys. Res.* **2002**, *107*, AAC 10−1−AAC 10−18.

(10) Kurtén, T.; Petäjä, T.; Smith, J.; Ortega, I. K.; Sipilä, M.; Junninen, H.; Ehn, M.; Vehkamäki, H.; Mauldin, L.; Worsnop, D. R.; et al. The effect of H_2SO_4−amine clustering on chemical ionization mass spectrometry (CIMS) measurements of gas-phase sulfuric acid. *Atmos. Chem. Phys.* **2011**, *11*, 3007−3019.

(11) Jiang, J.; Zhao, J.; Chen, M.; Eisele, F. L.; Scheckman, J.; Williams, B. J.; Kuang, C.; McMurry, P. H. First Measurements of Neutral Atmospheric Cluster and 1−2 nm Particle Number Size Distributions During Nucleation Events. *Aerosol Sci. Technol.* **2011**, *45*, 45:ii−v.

(12) Jokinen, T.; Sipilä, M.; Junninen, H.; Ehn, M.; Lönn, G.; Hakala, J.; Petäjä, T.; Mauldin, R. L., III.; Kulmala, M.; Worsnop, D. R. Atmospheric sulphuric acid and neutral cluster measurements using CI-APi-TOF. *Atmos. Chem. Phys.* **2012**, *12*, 4117−4125.

(13) Su, T.; Bowers, M. T. Theory of ion-polar molecule collisions. Comparison with experimental charge transfer reactions of rare gas ions to geometric isomers of diuorobenzene and dichloroethylene. *J. Chem. Phys.* **1973**, *58*, 3027.

(14) Su, T.; Chesnavich, W. J. Parametrization of the ion-polar molecule collision rate constant by trajectory calculations. *J. Chem. Phys.* **1982**, *76*, 5183.

(15) McGrath, M. J.; Olenius, T.; Ortega, I. K.; Loukonen, V.; Paasonen, P.; Kurtén, T.; Kulmala, M.; Vehkamäki, H. Atmospheric Cluster Dynamics Code: A exible method for solution of the birth−death equations. *Atmos. Chem. Phys.* **2012**, *12*, 2345−2355.

(16) Olenius, T.; Kupiainen-Määttä, O.; Ortega, I. K.; Kurtén, T.; Vehkamäki, H. Free energy barrier in the growth of sulfuric acid-ammonia and sulfuric acid-dimethylamine clusters. *J. Chem. Phys.* **2013**, *139*, 084312.

(17) Shampine, L.; Reichelt, M. The MATLAB ODE Suite. *SIAM J. Sci. Comp.* **1997**, *18*, 1−22.

(18) Haynes, W. M. Ed. *CRC Handbook of Chemistry and Physics*, 93th ed., Internet Version; CRC Press/Taylor and Francis: Boca Raton, FL, 2013.

(19) DePuy, C. H.; Gronert, S.; Mullin, A.; Bierbaum, V. M. Gas-Phase S_N2 and E2 Reactions of Alkyl Halides. *J. Am. Chem. Soc.* **1990**, *112*, 8650−8655.

(20) Zhao, J.; Zhang, R. Proton transfer reaction rate constants between hydronium ion (H_3O^+) and volatile organic compounds. *Atmos. Environ.* **2004**, *38*, 2177−2185.

(21) Kupiainen, O.; Ortega, I. K.; Kurtén, T.; Vehkamäki, H. Amine substitution into sulfuric acid - ammonia clusters. *Atmos. Chem. Phys.* **2012**, *12*, 3591−3599.

(22) Su, T. Parametrization of kinetic energy dependences of ion−polar molecule collision rate constants by trajectory calculations. *J. Chem. Phys.* **1994**, *100*, 4703.

(23) Eichelberger, B. R.; Snow, T. P.; Bierbaum, V. M. Collision Rate Constants for Polarizable Ions. *J. Am. Soc. Mass. Spectrom.* **2003**, *14*, 501−505.

(24) Ortega, I. K.; Kupiainen, O.; Kurtén, T.; Olenius, T.; Wilkman, O.; McGrath, M. J.; Loukonen, V.; Vehkamäki, H. From quantum chemical formation free energies to evaporation rates. *Atmos. Chem. Phys.* **2012**, *12*, 225−235.

(25) Bzdek, B. R.; DePalma, J. W.; Ridge, D. P.; Laskin, J.; Johnston, M. V. Fragmentation Energetics of Clusters Relevant to Atmospheric New Particle Formation. *J. Am. Chem. Soc.* **2013**, *135*, 3276−3285.

(26) Becke, A. D. Density-functional thermochemistry. III. The role of exact exchange. *J. Chem. Phys.* **1993**, *98*, 5648−5652.

(27) Montgomery, J. A., Jr.; Frisch, M. J.; Ochterski, J. W.; Petersson, G. A. A complete basis set model chemistry. VI. Use of density functional geometries and frequencies. *J. Chem. Phys.* **1999**, *110*, 2822−2827.

(28) Frisch, M. J.; Trucks, G. W.; Schlegel, H. B.; Scuseria, G. E.; Robb, M. A.; Cheeseman, J. R.; Scalmani, G.; Barone, V.; Mennucci, B.; Petersson, G. A. et al. Gaussian 09, Revision A.01. 2009.

(29) Christiansen, O.; Koch, H.; Jørgensen, P. The second-order approximate coupled cluster singles and doubles model CC2. *Chem. Phys. Lett.* **1995**, *243*, 409−418.

(30) Hättig, C.; Weigend, F. CC2 excitation energy calculations on large molecules using the resolution of the identity approximation. *J. Chem. Phys.* **2000**, *113*, 5154−5161.

(31) Dunning, T. H., Jr.; Peterson, K. A.; Wilson, A. K. Gaussian basis sets for use in correlated molecular calculations. X. The atoms aluminum through argon revisited. *J. Chem. Phys.* **2001**, *114*, 9244−9253.

(32) Ahlrichs, R.; Bär, M.; Häser, J.; Horn, H.; Kälmel, C. Electronic structure calculations on workstation computers: The program system TURBOMOLE. *Chem. Phys. Lett.* **1989**, *162*, 165−169.

(33) Curtiss, L. A.; Redfern, P. C.; Raghavachari, K.; Rassolov, V.; Pople, J. A. Gaussian-3 theory using reduced Moller-Plesset order. *J. Chem. Phys.* **1999**, *109*, 4703.

(34) Perdew, J. P.; Wang, Y. Accurate and Simple Analytic Representation of the Electron Gas Correlation Energy. *Phys. Rev. B* **1992**, *45*, 13244−13249.

(35) Mclean, A. D.; Chandler, G. S. Contracted Gaussian-basis sets for molecular calculations. 1. 2nd row atoms, Z = 1118. *J. Chem. Phys.* **1980**, *72*, 5639−5648.

(36) Krishnan, R.; Binkley, J. S.; Seeger, R.; Pople, J. A. Self-Consistent Molecular Orbital Methods. 20. Basis set for correlated wave-functions. *J. Chem. Phys.* **1980**, *72*, 650−654.

(37) Leverentz, H. R.; Siepmann, J. I.; Truhlar, D. G.; Loukonen, V.; Vehkamäki, H. Energetics of Atmospherically Implicated Clusters Made of Sulfuric Acid, Ammonia, and Dimethyl Amine. *J. Phys. Chem. A* **2013**, *117*, 3819−3825.

(38) Nadykto, A. B.; Yu, F.; Herb, J. Towards understanding the sign preference in binary atmospheric nucleation. *Phys. Chem. Chem. Phys.* **2008**, *10*, 7073−7078.

(39) Nadykto, A. B.; Yu, F.; Herb, J. Effect of Ammonia on the Gas-Phase Hydration of the Common Atmospheric Ion HSO_4^-. *Int. J. Mol. Sci.* **2008**, *9*, 2184−2193.

(40) Herb, J.; Xu, Y.; Yu, F.; Nadykto, A. B. Large Hydrogen-Bonded Pre-nucleation $(HSO_4^-)(H_2SO_4)_m(H_2O)_k$ and $(HSO_4^-)(NH_3)$-$(H_2SO_4)_m(H_2O)_k$ Clusters in the Earth's Atmosphere. *J. Phys. Chem. A* **2013**, *117*, 133−152.

(41) Davidson, J. A.; Fehsenfeld, F. C.; Howard, C. J. The heats of formation of NO_3^- and NO_3^- association complexes with HNO_3 and HBr. *Int. J. Chem. Kinet.* **1977**, *9*, 17−29.
(42) Meot-Ner, M. M. M.; Lias, S. G. In *NIST Chemistry WebBook*; Linstrom, P. J., Mallard, W. G., Eds.; NIST Standard Reference Database Number 69; National Institute of Standards and Technology: Gaithersburg MD, 20899, 2013; Retrieved September 19, 2013.
(43) Lovejoy, E. R.; Curtius, J. Cluster Ion Thermal Decomposition (II): Master Equation Modeling in the Low-Pressure Limit and Fall-Off Regions. Bond Energies for HSO_4^- $(H_2SO_4)_x(HNO_3)_y$. *J. Phys. Chem. A* **2001**, *105*, 10874−10883.
(44) Partanen, L.; Pesonen, J.; Sjäholm, E.; Halonen, L. A rotamer energy level study of sulfuric acid. *J. Chem. Phys.* **2013**, *139*, 144311.
(45) Tanner, D. J.; Je!rson, A.; Eisele, F. L. Selected ion chemical ionization mass spectrometric measurement of OH. J. *Geophys. Res.* **1997**, *102*, 6415−6425.
(46) Parmar, R. S.; Satsangi, G. S.; Lakhani, A.; Srivastava, S. S.; Prakash, S. Simultaneous measurements of ammonia and nitric acid in ambient air at Agra (27°10′N and 78°05′E) (India). *Atmos. Environ.* **2001**, *35*, 5979.
(47) Sauer, C. G.; Pisano, J. T.; Fitz, D. R. Tunable diode laser absorption spectrometer measurements of ambient nitrogen dioxide, nitric acid, formaldehyde, and hydrogen peroxide in Parlier, California. *Atmos. Environ.* **2003**, *37*, 1583−1591.
(48) Acker, K.; Mäller, D.; Auel, R.; Wieprecht, W.; Kalaß, D. Concentrations of nitrous acid, nitric acid, nitrite and nitrate in the gas and aerosol phase at a site in the emission zone during ESCOMPTE 2001 experiment. *Atmos. Res.* **2005**, *74*, 507−524.
(49) Yacovitch, T. I.; Heine, N.; Brieger, C.; Wende, T.; Hock, C.; Neumark, D. M.; Asmis, K. R. Communication: Vibrational spectroscopy of atmospherically relevant acid cluster anions: Bisulfate versus nitrate core structures. *J. Chem. Phys.* **2012**, *136*, 241102.
(50) Dal Maso, M.; Hyvärinen, A.; Komppula, M.; Tunved, P.; Kerminen, V.-M.; Lihavainen, H.; Viisanen, Y.; Hansson, H.-C.; Kulmala, M. Annual and interannual variation in boreal forest aerosol particle number and volume concentration and their connection to particle formation. *Tellus B* **2008**, *60*, 495−508.
(51) Almeida, J.; Schobesberger, S.; Kärten, A.; Ortega, I. K.; Kupiainen-Määttä, O.; Praplan, A. P.; Adamov, A.; Amorim, A.; Bianchi, F.; Breitenlechner, M.; et al. Molecular understanding of sulphuric acid−amine particle nucleation in the atmosphere. *Nature* **2013**, *502*, 359−363.